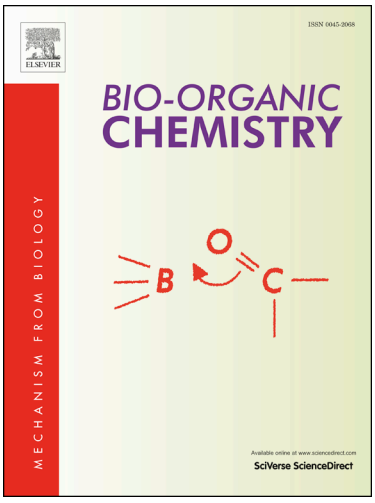

Targeting Microbial Resistance: Synthesis, Antibacterial Evaluation, DNA Binding and Modeling Study of New Chalcone-Based Dithiocarbamate Derivatives

Marwa Ayman, Shahenda M. El-Messery, Elsayed E. Habib, Sara T. Al-Rashood, Abdulrahman A. Almehizia, Hamad M. Alkahtani, Ghada S. Hassan

PII: S0045-2068(18)30751-X
DOI: https://doi.org/10.1016/j.bioorg.2019.01.001
Reference: YBIOO 2705

To appear in: *Bioorganic Chemistry*

Received Date: 21 July 2018
Revised Date: 29 December 2018
Accepted Date: 1 January 2019

Please cite this article as: M. Ayman, S.M. El-Messery, E.E. Habib, S.T. Al-Rashood, A.A. Almehizia, H.M. Alkahtani, G.S. Hassan, Targeting Microbial Resistance: Synthesis, Antibacterial Evaluation, DNA Binding and Modeling Study of New Chalcone-Based Dithiocarbamate Derivatives, *Bioorganic Chemistry* (2019), doi: https://doi.org/10.1016/j.bioorg.2019.01.001

Targeting Microbial Resistance: Synthesis, Antibacterial Evaluation, DNA Binding and Modeling Study of New Chalcone-Based Dithiocarbamate Derivatives

Marwa Ayman[1], Shahenda M. El-Messery[2#], Elsayed E. Habib[3,4], Sara T. Al-Rashood[5], Abdulrahman A. Almehizia[5], Hamad M. Alkahtani[5], Ghada S. Hassan[6*]

[1]Faculty of Pharmacy, Mansoura University, P.O.Box 35516, Mansoura, Egypt
[2]Department of Pharmaceutical Organic Chemistry, Faculty of Pharmacy, Mansoura University, P.O.Box 35516, Mansoura, Egypt
[3]Department of Pharmaceutics and Pharmaceutical Technology, College of Pharmacy, Taibah University, Almadinah Almunawwarah, 344, Saudi Arabia.
[4]Department of Microbiology, Faculty of Pharmacy, Mansoura University, Mansoura 35516, Egypt
[5]Department of Pharmaceutical Chemistry, College of Pharmacy, King Saud University, Riyadh, 11451, Saudi Arabia.
[6]Department of Medicinal Chemistry, Faculty of Pharmacy, Mansoura University, P.O.Box 35516, Mansoura, Egypt

* Corresponding author. *Department of Medicinal Chemistry, Faculty of Pharmacy, Mansoura University,P.O.Box 35516, Mansoura, Egypt. E-mail:* ghadak25@yahoo.com. Tel, Fax: +20-50-2200242
\# Corresponding author. *Department of Pharmaceutical Organic Chemistry, Faculty of Pharmacy, Mansoura University, P.O.Box 35516, Mansoura, Egypt. E-mail: selmessery@gmail.com* Tel, Fax: +20-50-2200242

Abstract

New dithiocarbamate chalcone-based derivatives were synthesized, their structures were elucidated using different spectroscopic techniques. They were subjected to antimicrobial screening against selected *Gram negative* bacteria focusing on microbial resistance. Bacterial resistance was targeted via phosphoethanolamine transferase enzyme. Most of the synthesized compounds showed equal or higher activity to colistin standard. Compound **24** proved to be the most active candidate with MIC of 8 µg/ml against both Ps12 and K4 and MBC of 32 µg/ml against Ps12 and 16 µg/ml against K4 Molecular docking study showed that **20, 22,24** and **25** had good binding affinity with active site residues *via* Thr280. DNA macromolecule was further targeted. Compounds **28** and **34** were recorded to have better DNA binding than doxurubucin with IC_{50} of 27.48 and 30.97 µg/ml respectively, suggesting that it could have a role in their higher antibacterial effect. Their docking into DNA has shown a clear intercalation matching with antibacterial data. Pharmacokinetics parameters of active compounds showed that they have better absorption through GIT.

Keywords: Synthesis; dithiocarbamate chalcones; Bacterial resistance; Molecular docking studies.

1. Introduction

Resistance of pathogenic bacteria towards already existing antibiotics has appeared extensively more and more during the last decade. [1] Trials have been applied to face such resistance, either through the use of antibiotic combinations, or through discovering new antibiotics that help repelling the infectious diseases or through the use of natural products to decrease the effects of such drugs on human bodies.[2, 3] The discovery of new lines of treatment may involve the use of new agents having new modes of action, or combination of conventional antibiotics and suitable agents to treat the infections produced by these pathogens. [3] The polymyxin colistin is a key antibiotic that acts as last resort for infections treatment caused by multidrug resistant pathogens [4]. It acts through binding of its positively-charged cyclic peptide to the negatively charged Lipid A headgroup. The colistin key resistance mechanism occurs through the production of MCR-1 which is a plasmid-encoded phosphoethanolamine transferase (PEA transferase) and it was isolated from many pathogens such as *Escherichia coli* and *Klebsiella pneumoniae.* MCR-1 catalyses the transfer of positively charged PEA transferase onto lipid A, which is incorporated to the outer membrane, and consequently decreases the outer membrane negative charge and finally prevent the action of colistin producing pathogen resistance to the latter.[4] So, to decrease the pathogen resistance to colistin, blocking of MCR-1 is essential. Chalcones are compounds with simple structure that are formed through Claiesen-Schmidt reaction between aldehydes and active methylene group in ketone under basic conditions. It is considered to be important part of many biologically active agents. Chalcones and their derivatives exert many activities such as antihypertensive, antitumor, anti-inflammatory and antioxidant effects.[5] Naturally-occuring chalcones usually contain a variety of substituents such as hydroxyl, methoxy, or phenyl groups, on the other hand, synthetic derivatives contain other substitution such as halogen, nitro, and the benzene ring can be substituted by other aryl or heteroaryl rings. [6] Different dithiocarbamate (DTC) ligands either connected to Zn (II) and Ni (II) complexes [7] or to different amines [8] have showed significant antimicrobial activity[9]. Moreover dithiocarbamate moiety was also included in carbapenem antibiotic chart 1 (A) and also in different metallic amtimicrobial compounds as in chart 1 (B).[10, 11]

Moreover, it was concluded that the molecular hybridization technique of DTC with another pharmacophore may be a successful method to discover a new promising antimicrobial candidate of different physicochemical properties. Accordingly, they can be considered as lead to be used as antimicrobial agents. [12]

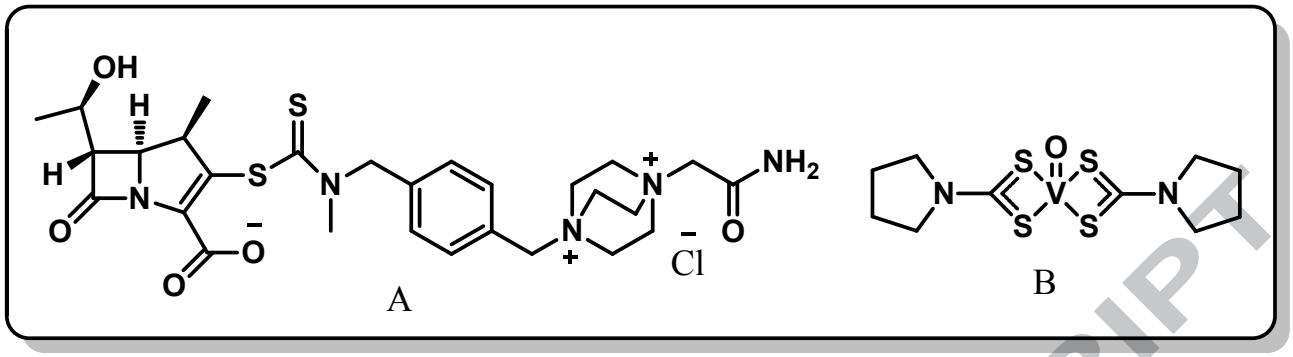

Chart 1: Structures of antimicrobial dithiocarbamates

In the present work, and in a continuation of our previous efforts to design and synthesize small molecules of potential antimicrobial effect [13-16], a series of chalcone-based dithiocarbamates derivatives has been designed using molecular hybridization technique gathering chalcones, ditiocarbamate and amine moieties (chart 2) . They have been synthesized then characterized by spectral data including IR, ^{1}HNMR, ^{13}CNMR, and mass spectrometry. The microbial resistance was targeted through antibacterial evaluation of highly resistant *gram-negative* bacteria such as *Pseudomonas aeruginosa* and *Klebsiella pneumonia*. The minimum inhibitory concentrations (MIC) and minimum bactericidal concentrations (MBC) of the synthesized compounds were determined. To study the mechanism of the antimicrobial activity obtained, two molecular targets were considered PEA transferase inhibition as a first target focusing on bacterial resistance. A second goal targeting DNA binding affinity relying on chalcone fragment of our compounds was attained. Docking studies have been applied to understand the obtained results. ADMET study for the most active compounds was also determined .

.

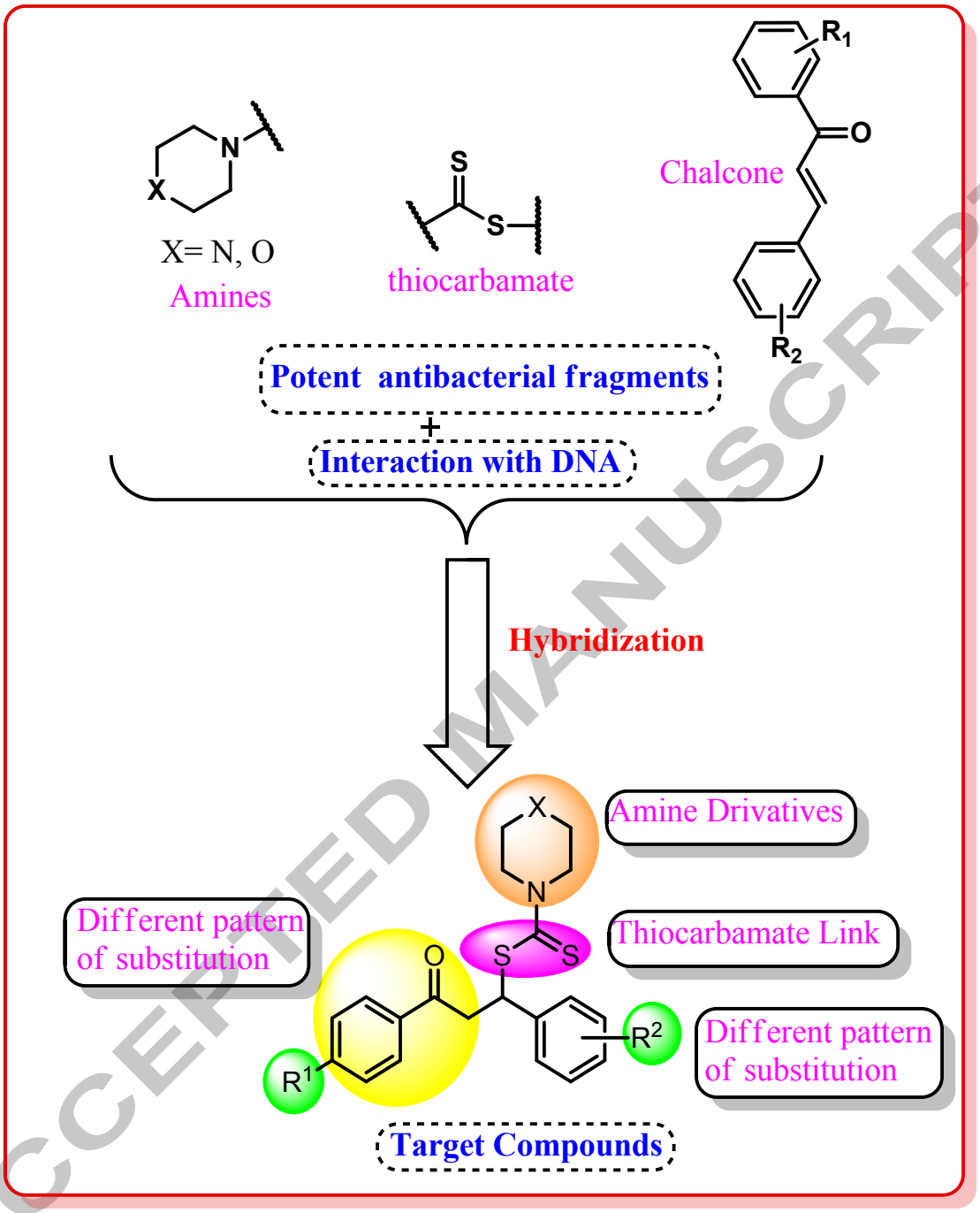

Chart 2: Representation of different active part of newly synthesized compounds

2. Results and Discussion

2.1. Chemistry

The synthetic procedures of the target compounds were illustrated in Scheme 1. Starting with condensation reaction between acetophenone derivatives (**1,2**) and substituted aldehyde (**3-7**) to yield the α,β-unsaturated compounds (**8-17**). [17a,b] The final compounds were obtained through two step reaction, firstly, the reaction of compounds **8-17** with carbon disulphide in ethanol [17c], followed by reaction of the resultant products –used without purification- with secondary amine either morpholine or 1-benzyl piperazine producing the final compounds in good yields. (Scheme 1, Table 1). The structures of the synthesized compounds have been confirmed through spectral data including IR, ^{1}HNMR, ^{13}CNMR and mass spectrometry. All synthesized compounds have shown a characteristic C=S band in 950-1050 cm^{-1} range proving the inclusion of DCM group in all compounds accompanied by characteristic N-CS band around 1530 cm^{-1}. ^{1}HNMR spectral data for compounds **20-29** showed the appearance of morpholine protons either in the form of multiplets ranging from 2.34 – 3.50 or in the form of two triplets ranging from 3.07 – 3.43 and 3.59 – 3.73. Similarly, for compounds **30-39**, the appearance of two benzylic protons in addition to the piperazine protons confirmed the structures of the target compounds. The benzylic protons appeared in range of 3.43 – 4.22, and the piperazine protons appeared either as multiplet peaks at range of 3.10 – 3.48, or as two triplets appearing at 3.10 – 3.11 and 3.52 - 3.58. The mass spectral data are consistent with the synthesized products through the appearance of M^{+} for each compound under investigation.

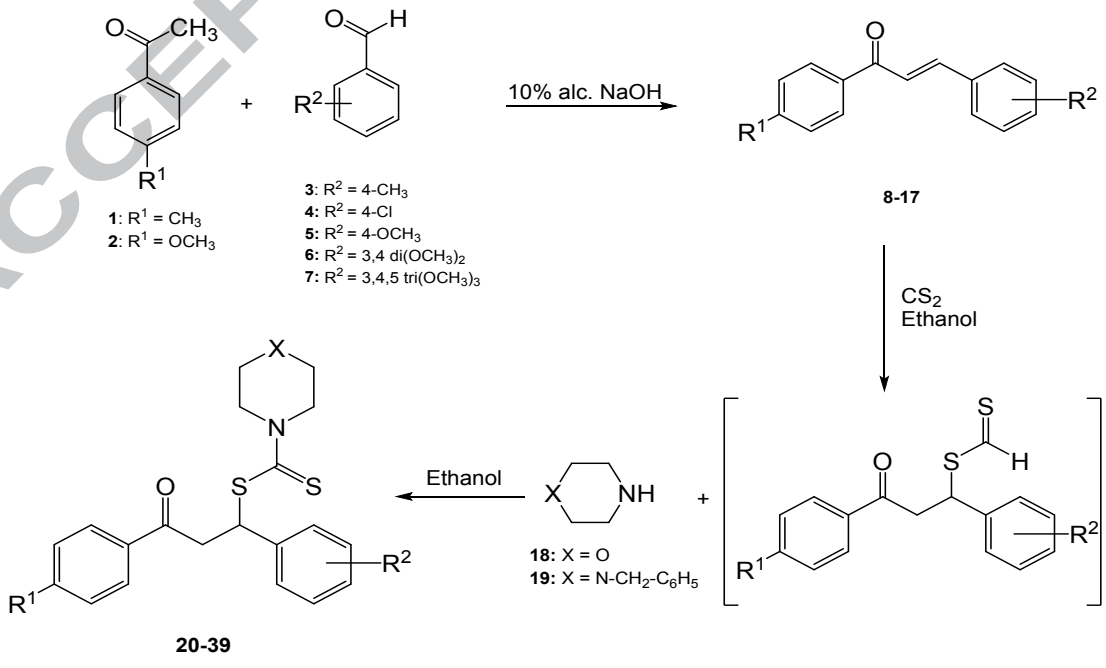

Scheme 1: Synthesis of the target compounds 20-39

Table 1: The physiochemical properties of the synthesized compounds 20-39

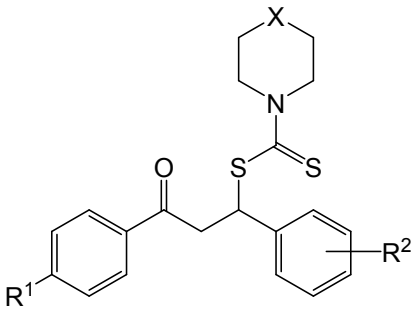

20-39

Comp. no.	R^1	R^2	X	% Yield	Mp. °C	Molecular Formula[a]
20	CH_3	CH_3	O	75	172-175	$C_{22}H_{25}NO_2S_2$ (399.57)
21	CH_3	Cl	O	55	152-155	$C_{21}H_{22}ClNO_2S_2$ (419.98)
22	CH_3	OCH_3	O	62	186-189	$C_{22}H_{25}NO_3S_2$ (415.57)
23	CH_3	di- OCH_3	O	88	142-146	$C_{23}H_{27}NO_4S_2$ (445.59)
24	CH_3	tri- OCH_3	O	49	200-203	$C_{24}H_{29}NO_5S_2$ (475.62)
25	OCH_3	CH_3	O	90	179-182	$C_{22}H_{25}NO_3S_2$ (415.57)
26	OCH_3	Cl	O	57	169-171	$C_{21}H_{22}ClNO_3S_2$ (435.98)
27	OCH_3	OCH_3	O	76	194-167	$C_{22}H_{25}NO_4S_2$ (431.57)
28	OCH_3	di- OCH_3	O	69	160-163	$C_{23}H_{27}NO_5S_2$ (461.59)
29	OCH_3	tri- OCH_3	O	80	198-201	$C_{24}H_{29}NO_6S_2$ (491.62)
30	CH_3	CH_3	N-CH_2-C_6H_5	84	133-136	$C_{29}H_{32}N_2OS_2$ (488.71)
31	CH_3	Cl	N-CH_2-C_6H_5	93	176-179	$C_{28}H_{29}ClN_2OS_2$ (509.12)
32	CH_3	OCH_3	N-CH_2-C_6H_5	61	159-161	$C_{29}H_{32}N_2O_2S_2$ (504.71)
33	CH_3	di- OCH_3	N-CH_2-C_6H_5	74	155-158	$C_{30}H_{34}N_2O_3S_2$ (534.73)
34	CH_3	tri- OCH_3	N-CH_2-C_6H_5	59	166-169	$C_{31}H_{36}N_2O_4S_2$ (564.76)
35	OCH_3	CH_3	N-CH_2-C_6H_5	66	138-141	$C_{29}H_{32}N_2O_2S_2$ (504.71)
36	OCH_3	Cl	N-CH_2-C_6H_5	83	149-152	$C_{28}H_{29}ClN_2O_2S_2$ (525.12)
37	OCH_3	OCH_3	N-CH_2-C_6H_5	54	211-215	$C_{29}H_{32}N_2O_3S_2$ (520.71)
38	OCH_3	di- OCH_3	N-CH_2-C_6H_5	89	191-193	$C_{30}H_{34}N_2O_4S_2$ (550.73)
39	OCH_3	tri- OCH_3	N-CH_2-C_6H_5	79	182-184	$C_{31}H_{36}N_2O_5S_2$ (580.76)

[a]Analysed for C,H,N; results were within ± 0.4 % of the theoretical values for the formulae given

2.2. *In vitro* antibacterial activity

The synthesized compounds were tested for their *in vitro* antibacterial activity against selected multidrug-resistant *Gram negative* clinical isolate, *Pseudomonas aeruginosa* (Ps12) and *Klebsiella pneumoniae* (K4). The primary screen was carried out using the agar disc-diffusion method using Müller-Hinton agar medium. The results of the preliminary antimicrobial testing of the synthesized compounds and the antibacterial activity of the selected compound Colistin are shown in Table 2. The results revealed that the majority of the synthesized compounds showed varying degrees of inhibition against the tested microorganisms. The Bacterial isolates showed a moderate resistant to colistin which considered to be more effective against the multidrug-resistant *Gram negative* bacteria. Compounds

20, 22, 25- 28, 33 - 37 showed good activity against the bacterial isolate. The most active compound **24** showed a very strong activity against both multidrug-resistant Gram *negative* clinical isolate, *Pseudomonas aeruginosa* (Ps12) and *Klebsiella pneumoniae* (K4). The MIC and MBC for the most active compounds against the same microorganism used in the primary screening was carried out using the micro dilution susceptibility method in

Müller-Hinton Broth as shown in Table 3. Compound **24** showed very good MIC and MBC against tested organisms. This results may explain that the multidrug-resistant Gram *negative* isolate produce phosphoethanolamine transferase enzyme that is responsible for the resistant of these bacteria to the most potent antibacterial agent, colistin and the tested compounds may be inhibited this enzyme so the bacteria become highly sensitive to the tested compounds.

Table 2: Antibacterial activity of tested compounds (200 µg/8 mm disc) against selected multidrug-resistant *Gram negative* clinical isolate, *Pseudomonas aeruginosa* (Ps12) and *Klebsiella pneumoniae* (K4).

	Inhibition zone diameter (mm)	
Comp. No.	*Pseudomonas aeruginosa* (Ps12)	*Klebsiella pneumoniae* (K4)
20	**28**	**26**
21	10	15
22	**18**	**22**
23	15	**20**
24	**30**	**32**
25	**24**	**25**
26	**25**	**24**
27	**23**	**22**
28	**22**	**21**
29	15	**20**
30	12	12
31	10	11
32	10	10
33	**18**	**24**
34	**23**	**20**
35	**18**	**20**
36	**24**	**25**
37	**18**	**22**
38	10	11
39	**17**	**22**
Colistin	18	14

Not active (8 mm), Weak activity (8-12 mm), Moderate activity (12-18 mm), Strong activity (> 18 mm). Solvent: DEMSO (8 mm).

Table 3: The Minimal Inhibitory Concentrations (MIC, µg/ml) and Minimal Bactericidal Concentrations (MBC µg/ml) of compounds **20, 22, 24, 25. 26, 27, 28 33, 34 35, 36 and 37** in comparison with the broad spectrum antibacterial drug, Colistin against selected multidrug-resistant *Gram negative* clinical isolate, *Pseudomonas aeruginosa* (Ps12) and *Klebsiella pneumoniae* (K4).

Comp. No.		***Pseudomonas aeruginosa* (Ps12)**	***Klebsiella pneumoniae* (K4)**
20	**MIC**	16	32
	MBC	32	> 64
22	**MIC**	> 64	64
	MBC	ND	ND
24	**MIC**	8	8
	MBC	32	16
25	**MIC**	32	**16**
	MBC	ND	64
26	**MIC**	32	32
	MBC	64	> 64
27	**MIC**	32	64
	MBC	ND	ND
28	**MIC**	32	32
	MBC	> 64	ND
33	**MIC**	> 64	32
	MBC	ND	ND
34	**MIC**	32	64
	MBC	> 64	ND
35	**MIC**	> 64	> 64
	MBC	ND	ND
36	**MIC**	32	16
	MBC	> 64	64
37	**MIC**	> 64	32
	MBC	ND	> 64
Colistin	**MIC**	> 64	> 64
	MBC	ND	ND

ND: Not Determined.

2.3. DNA Binding Assay

DNA is the pharmacologic target of many antimicrobial drugs currently in clinical use or in advanced clinical trials. It was proved that small molecules can act as potent antimicrobials *via* DNA intercalation. A colourimetric methyl green DNA displacement assay method was used to reversibly bind to DNA, and the colored complex is stable at neutral pH, whereas free methyl green fades at this pH value. [18] Incubation for 24 h, in the buffer was used for displacement reactions in this study, results in virtually a complete loss of methyl green absorbance. In this study, compounds **20**, **28**, **34** ,showed the highest affinity to DNA, compounds **20** and **23** with even equipotent activity to doxorubusin while compounds **21** and **31** are the least DNA binding compounds other compounds does not show DNA binding affinity although some of them have potent antibacterial activity which could be attributed to another mechanism. (Table 4) Some of These results are in accordance with the antimicrobial screening data and explain them,suggesting that binding with DNA may contribute the activity of these compounds against bacterial infections.

Table 4: DNA/methyl green colourimetric assay of the DNA-binding compounds

DNA-active compound	DNA/methyl green (IC_{50} µg/ml)
DOX	31.27±1.8
20	39.70±2.1
21	81.12±3.5
22	44.81±2.3
23	36.14±1.9
28	27.48±1.5
29	63.24±2.7
30	78.03±3.2
31	83.26±3.9
34	30.97±1.7
35	48.20±2.4
38	67.35±3.1
39	55.79±2.6

2.3 Molecular Docking Study

Molecular docking and virtual screening have become an integral part of many modern structure-based drug discovery efforts. The binding of small molecule ligands to large protein targets is central to numerous biological processes. The accurate prediction of the binding modes between the ligand and protein (the docking problem) is of fundamental importance in modern structure-based drug design. [19, 20] MOE as a flexible docking program facilitates the prediction of favorable protein–ligand complex structures with reasonable accuracy and speed. Phosphoethanolamine (PEA) trasferase and DNA were targeted for docking to suggest the mechanism of antibacterial action

2.3.1 Phosphoethanolamine transferase enzyme:

Binding affinities and orientation of compounds at the calculated active site of the PEA trasferase enzyme were determined. The protein–ligand complex was constructed based on the X-ray structure PEA transferases belong to the alkaline phosphatase super-family. Many multidrug resistance (MDR) *gram-negative* bacteria possess multiple members of this family of enzymes that are engaged in the decoration of lipid A or the conserved inner core of the lipopolysaccharide [21,22]. To investigate possible binding mode interactions, molecular docking studies were performed by domly docking representative active antimicrobial compounds of our study into PEA transferase enzyme. The recently-solved X-ray crystal structure of the PDB ID: 5FGN [23] was used as the starting model. Structure of a lipid A PEA transferase suggests how conformational changes govern substrate binding . The corresponding cocrystallized ligand show a network of hydrogen bonding with with Thr 280 Gln 91, Ala281, Asn, 106 and His 465 amino acid residues .(Fig. 1) It was reported that Thr.280 is a considered a key aminoacid Especially concering binding. [23] All the compounds were found to exhibit binding poses similar to those of cocrystallized ligands occupying the binding cavity and, to varying extents, the gorge connecting it . **Compound 20** was recorded to occur in active site (characterized by our modeling experiment) binding to Thr 280 and His 465 by hydrogen bonding between carbonyl oxygen and Met 103 and aromatic cationic bonding to Val 107 (Fig 2). **Compound 22** showed Hydrogen bonding via thiocarbonyl sulphur to Thr 110 and another one through sulphur atom to Asn 106 .Additional hydrogen bond is detected *via* morpholine ring oxygen to His 465 (Fig 3) while **compound 24** has produced A net work of hydrogen bonding between carbon and oxygen and both Asn 108 and Met 103 occupying all active site .(Fig. 4, 5) In addition to the sulphur atom contribution by both hydrogen bonding tp Gln 91 and a arene-hydrogen tp Gln 91 too **compound, 25** were connected to the enzyme via Thr 280, His 453, Ala 281, Ser 279 and His 465 through hydrogen bonding (Fig. 6). The obtained results may suggest that the antibacterial activity of compounds **20, 22, 24** and **25** may occur via PEA transferase inhibition.

Figure 1: 2D binding mode and residues involved in the recognition of reference cocrystalized ligand in phosphoethanolamine (PEA) transferase active site

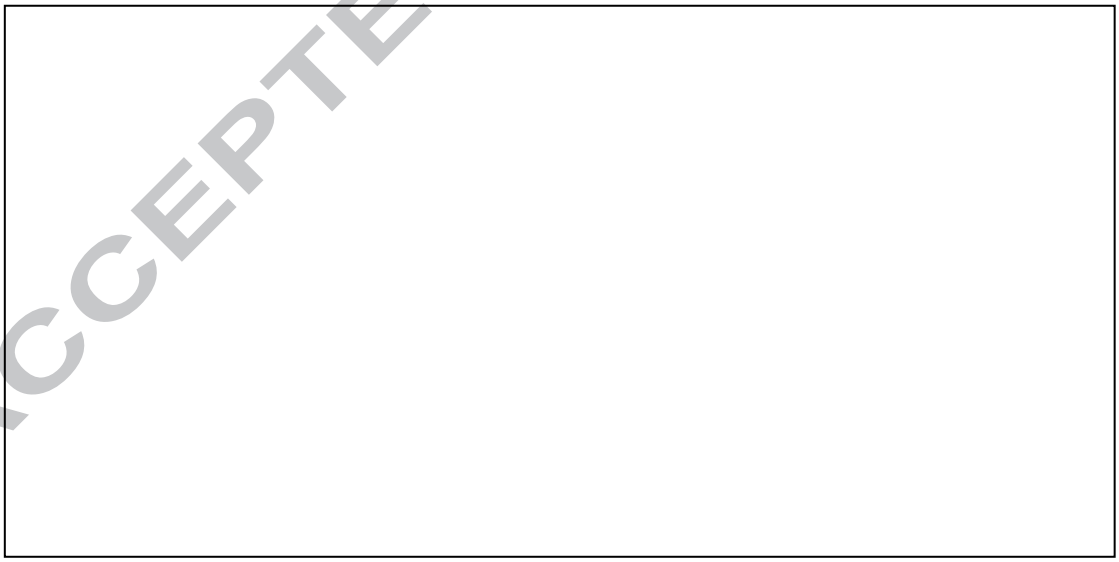

Figure 2: 2D binding mode and residues involved in the recognition of **20** in PEA transferase active site .

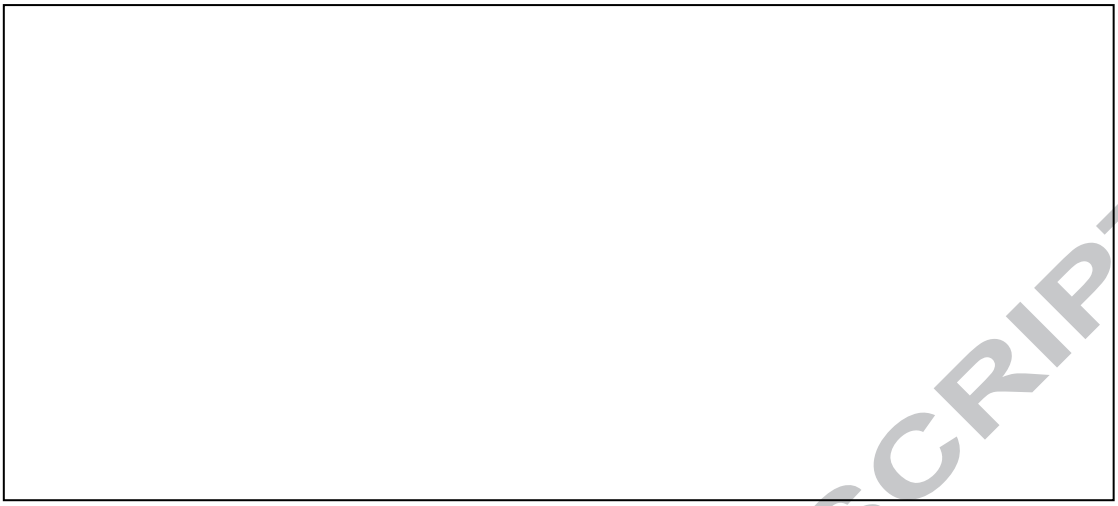

Figure 3: 2D binding mode and residues involved in the recognition of **22** in PEA transferase active site .

Figure 4: 2D binding mode and residues involved in the recognition of **24** in PEA trasferase active site

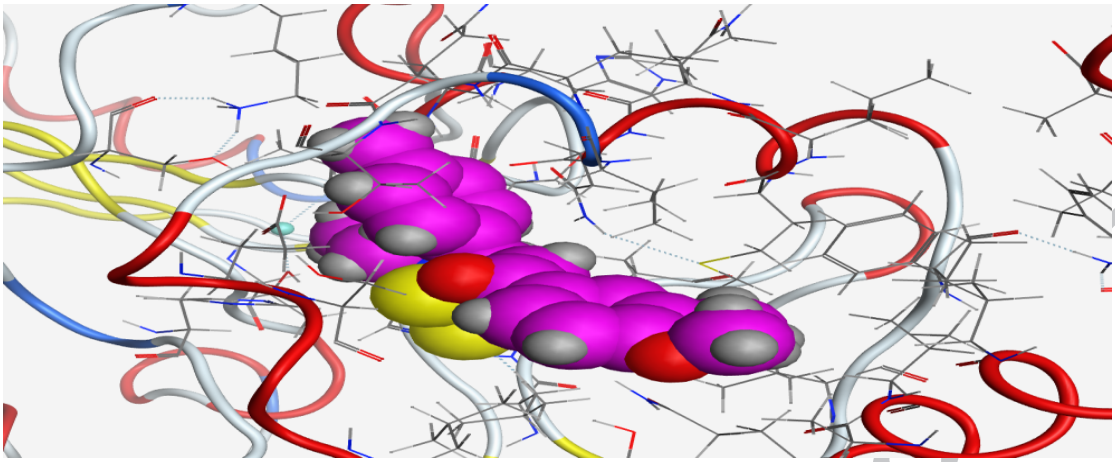

Figure 5: The aligned conformations of the most active compound **24** (IC_{50} 0.004 μM); occupying phosphoethanolamine transferase active site

Figure 6: 2D binding mode and residues involved in the recognition of **25** in PEA transferase active site.

2.3.2 Molecular Modeling Study & DNA Binding :

Molecular docking technique has been used as a tool to understand the practical results obtained from DNA binding assay method to present a mechanistic study. They were docked into the binding site region of the DNA mainly in a noncovalent fashion [13]. In the present study X-ray crystallographic structure of the DNA dodecamerd (CGCAAATTTGCG) with a bifurcated hydrogen-bonded conformation of the AT base pairs and its complex with distamycin A from the Protein Data Bank (PDB code: 2DND) for the docking study [15]. DNA-binding affinity, as well as the preferred orientation of the docking pose can be obtained from docking results. Doxorubicin formed a network of hydrogen bonds (Fig. 7a) and it occupied all the pocket intercalating between the two DNA strands (Fig. 7b). The lowest energy conformers of selected active and inactive DNA binders have been obtained using conformational search (Fig 8) to interpretate the results we got, the proposed binding

mode of the represented DNA active binders **28** IC_{50} 27.48±1.5 µg/ml and **34** IC_{50} 30.97±1.7 µg/ml showed that the aromatic planer moiety intercalates toward the minor groove between the double strands of DNA (Fig 9 a,b). Hence the antibacterial activity of these compounds could be attributed to DNA binding ability. On the other hand, the inactive candidates **21** and **31** were projecting out of the double strands interpretating their DNA lower binding affinity (Fig 9 c,d).

.

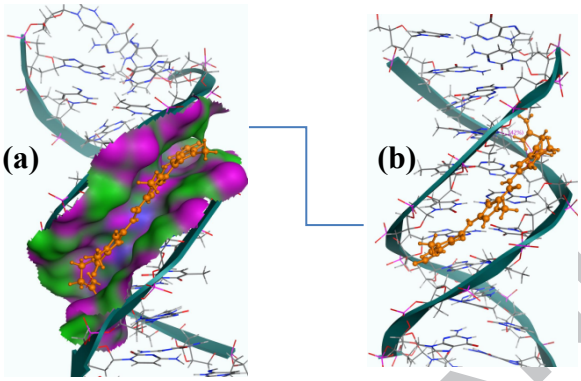

Figure 7 : DNA minor groove binding of (a) Distamycin (yellow) with DNA, DNA is shown in ribbon form. Distamycin, is shown in ball and cylinder form. Hydrogen-bonding (HB) interactions of with the DNA bases (dashed lines). Numbers indicate the percent of HB

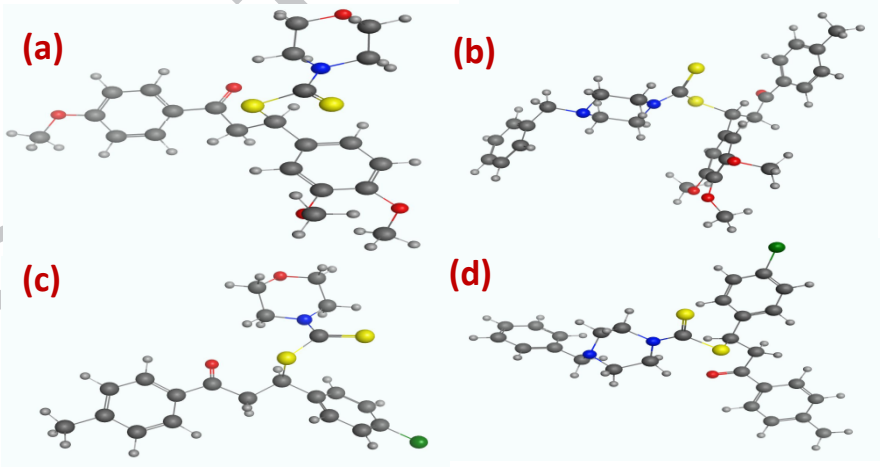

Figure 8: Lowest energy conformers of active compounds (a) **28** , (b) **34**, and the least active compounds (c) **21** and (d) **31** with balls and cylinders.

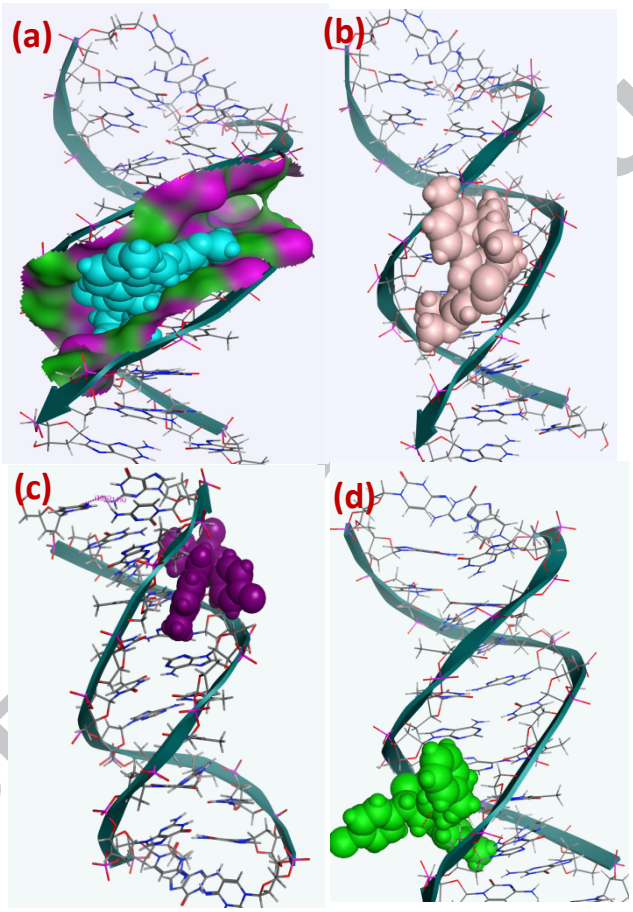

Figure 9: Close-up view of active candidates 28 (a), 34 (b) and inactive candidates 21 (c), 31 (d) binding in the DNA minor groove, highlighting the "isohelical" conformation of DNA active binders 28 and 34 to fit into minor groove

2.4 **ADMET Analysis**

The pharmacokinetic properties of most active antibacterial candidates of our study were calculated theoretically by the use of online application PreADME https://preadmet.bmdrc.kr. The results obtained revealed that all the tested compounds exerted excellent absorption through the intestine with HIA values exceeding 97.5 %, in contrast for the standard compound that has no absorption through the GIT because of its high polarity. In addition, they showed good binding with plasma protein that can give indication about the diffusion and availability of the tested compounds. Compound **24** exerted the best BBB penetration among the tested compounds; it has 10 times more penetration than the standard compound that can give privilege to be used for brain infection. The cell permeability of the compound **25** is higher than any other derivative. All the compounds proved to be non-carcinogen. (Table 5).

Table 5: ADMET profile for compounds **24 – 28** and **34**,**36** and the control drug Colistin

Comp.	HIA	PPB	BBB	MDCK	Carcinogenecity
24	98.99	91.33	0.31	2.070	Non-carcinogen
25	97.91	95.20	0.03	55.42	Non-carcinogen
26	97.71	96.09	0.11	34.59	Non-carcinogen
27	98.55	95.84	0.22	16.97	Non-carcinogen
28	99.19	93.30	0.37	1.370	Non-carcinogen
34	97.90	87.88	0.15	0.060	Non-carcinogen
36	98.16	90.18	0.07	5.29	Non-carcinogen
Colistin	0.00	43.97	0.03	0.04	Non-carcinogen

HIA : Human Intestinal Absorption, **PPB**: Plasma Protein Binding, **BBB**: Blood Brain Barrier, **MDCK**: Maden Darby Canine Kidney

2.5 **Structure-Activity Correlation**

In general, the synthesized compounds proved activity against the *gram-negative* microorganisms used in the study. Most of them proved to be active than the standard drug used (Colistin). According to the obtained antibacterial activity, most of the examined compounds revealed high degrees of inhibition toward the tested organisms. By taking a closer look, it was found that the morpholine analogs are the most potent series among the synthesized compounds; they exhibited potent activity higher than the standard drug Colistin with inhibition zone diameter against both *Pseudomonas aeruginosa* and *Klebsiela pneumoniae* ranging from **18** mm till reaching the maximum at **32** mm with the most potent derivative **24**. The latter compound is the most potent among all compounds with inhibition zone diameter of 30 and 32 mm against the mentioned organisms respectively. The presence of chloride atom decreased the activity of the analogs as in compounds **21** and **31** in both series, while the other substitutents such as methyl and methoxy are only effective in the N-benzyl piperazine series as in compounds **20** and **22**. Furthermore, it was observed that most of the active compounds were effective against *Klebsiela pneumonia* more than *Pseudomonas aeruginosa* with increased inhibition

zone diameters. In addition to compounds **25-28**. On the other hand, replacement of morpholine with benzyl piperazine retains the activity but with decrease in the potency as in compounds **33-37** and **39**. Furthermore, it was found that the presence of the chloride atom with mono-methoxy group is better for activity as in case of compounds **26** and **36**, while the presence of 2 methoxy groups leads to slight decrease of potency as in case of compounds **27** and **37**. It was also noticed that the introduction of more than methoxy group retains the activity towards *Klebsiella pneumonia* while it abolishes the activity towards *Pseudomonas aeruginosa* strains as in case of compounds **29, 38** and **39**. Moreover, the presence of methyl group either with the morpholine or the benzyl piperazine series completely abolishes the activity as in case of compounds **21, 30** and **31**.

3 Conclusion

A new series of chalcone-based dithiocarbamate derivatives was synthesized and evaluated for their antibacterial activity against resistant *gram-negative* bacteria named *Pseudomonas aeruginosa* (Ps12) and *Klebsiella pneumoniae* (K4). The results revealed the good activity of most of the synthesized compounds in addition to the presence of potent derivatives that have activity higher than the standard drug used in the antibacterial screening, Colistin. MIC and MBC for the active compounds were determined and they are consistent with the results obtained from the preliminary screening. Molecular DNA binding and PEA transferase enzyme were selected as targets for mechanism of action based on structure based fragments from one side and the resistance issue from another side respectively. Modeling studies revealed that compounds such as **20, 22, 24, and 25** have a good binding to PEA trasferase which may contribute to higher activity against the selected resistant strains *via* Thr 280 . Compounds **28 and 34** may excert their action *via* DNA intercalation as they have higher DNA binding affinity than doxorubicin itself. Data obtained was supported by antimicrobial screening and DNA binding assay in addition to docking study. Structure activity relationship has been performed. Pharmacokinitic properties gives a good optimizing data regarding the better bioavailabilty characters of synthesized compounds than colistin.

4 Experimental Section

The synthesis of the designed compounds was performed in Faculty of Pharmacy, Mansoura University, Mansoura, Egypt. The antimicrobial screening was conducted in the department of Micobiology, Faculty of Pharmacy, Mansoura University, Mansoura, Egypt. It was performed in comparison with the broad spectrum antibacterial drug, Colistin against selected multidrug-resistant *Gram negative* clinical isolate, *Pseudomonas aeruginosa* (Ps12) and *Klebsiella pneumoniae* (K4). Molecular docking experiments were performed using 'Molecular Operating Environment' software

on Core i7 workstation. Melting points (°C) were determined on Mettler FP80 melting point apparatus and are uncorrected. Microanalyses were performed on a Perkin-Elmer 240 elemental analyzer. All of the new compounds were analyzed for C, H and N and agreed with the proposed structures within ± 0.4% of the theoretical values.IR spectra were recorded in central lab of Fac. Of Pharmacy, Mansoura Uniersity. ^{1}H, ^{13}C-NMR were recorded on a Joel 500 MHz FT spectrometer; chemical shifts are expressed in δ ppm with reference to TMS. Mass spectral (MS) data were obtained on a Perkin Elmer, Clarus 600 GC/MS and Joel JMS-AX 500 mass spectrometers. Thin layer chromatography was performed on precoated (0.25 mm) silica gel GF_{254} plates (E. Merck, Germany), compounds were detected with 254 nm UV lamp. Silica gel (60–230 mesh) was employed for routine column chromatography separations. All the fine chemicals and reagents used were purchased from Aldrich Chemicals Co, USA.

4.1 Chemistry

4.1.1 1-(Substituted phenyl)-3-oxo-3-(4-substituted phenyl)propyl morpholine-4-carbodithioate **(20-29).**

A mixture of carbondisulfide (0.15 ml, 2.5 mM) and chalcone 8-17 (2.5 mM) was dissolved in dichloromethane (10 ml) and the solution was cooled to 0 oC in an ice bath. Morpholine (0.19 g, 2.25 mM) was slowly added and the reaction mixture was stirred at 0 oC for 30 min. Then, the solution was warmed to room temperature and stirred for another 24 h, and the reaction was monitored by TLC. After the end of the reaction, solvents were removed under vaccum and the residue was purified by column chromatography on silica gel (ethyl acetate–petroleum ether) affording compound dithiocarbamates (Table 1).

3-Oxo-1,3-di-p-tolylpropyl morpholine-4-carbodithioate (20) :

^{1}H-NMR (DMSO-d6); δ 1.04 (s, 3H, CH_3), 2.40 (s, 3H, CH_3), 3.38 (d, 2H, CH_2- C=O), 3.44 – 3.48 (m, 8H, morpholine-H), 4.29 (t, 1H, J = 9.5, benzylic-H), 7.00 (d, 2H, J = 8.5, Ar-H), 7.36 (d, 2H, J = 8.0, Ar-H), 7.84 (d, 2H, J = 8.5, Ar-H), 8.05 (d, 2H, J = 8.0, Ar-H). **^{13}C-NMR** δ 15.2, 20.4, 35.2, 49.1, 53.0, 54.8, 62.1, 63.2, 119.2, 120.4, 121.1, 126.0, 128.5, 130.7, 135.9, 137.4, 139.6, 140.7, 144.0, 146.2, 185.9, 194.6. **IR** (cm^{-1}): 1537 (N-CS), 1012 (C-S), **MS** *m/z* (%): 399.6 (15.2, M^+).

1-(4-Chlorophenyl)-3-oxo-3-(p-tolyl)propyl morpholine-4-carbodithioate (21):

^{1}H-NMR (DMSO-d_6); δ 1.03 (s, 3H, CH_3), 3.16 (d, 2H, $\underline{CH_2}$- C=O), 3.44-3.50 (m, 8H, morpholine-H), 4.32 (t, 1H, *J* = 9.5, benzylic-H), 7.37 (d, 2H, *J* = 7.5, Ar-H), 7.52 (d, 2H, *J* = 7.5, Ar-H), 7.94 (d, 2H, *J* = 8.5, Ar-H), 8.07 (d, 2H, *J* = 8.0, Ar-H). **^{13}C-NMR** δ 21.0, 35.9, 50.2, 53.1, 53.9, 60.9, 64.1,

120.7, 122.9, 124.1, 126.0, 129.3, 130.7, 132.1, 133.8, 135.0, 141.2, 144.6, 145.2, 179.2, 185.6. **MS** *m/z* (%): 419.9 (19.3, M^+).

1-(4-Methoxyphenyl)-3-oxo-3-(p-tolyl)propyl morpholine-4-carbodithioate (22)

^{1}H-NMR (DMSO-d_6); δ 1.04 (s, 3H, CH_3), 2.34 – 2.43 (m, 8H, morpholine-H), 2.48 (d, 2H, *J* = 3.0, $\underline{CH_2}$- C=O), 3.41 (s, 3H, OCH_3), 4.29 (t, 1H, *J* = 9.5, benzylic-H), 7.26 (d, 2H, *J* = 7.5, Ar-H), 7.36 (d, 2H, *J* = 8.0, Ar-H), 7.77 (d, 2H, *J* = 8.0, Ar-H), 8.05 (d, 2H, *J* = 8.5, Ar-H). **^{13}C-NMR** δ 23.5, 34.7, 49.8, 53.3, 54.6, 55.6, 63.1, 65.2, 119.2, 120.7, 121.6, 123.8, 126.9, 129.1, 130.6, 133.9, 136.0, 139.4, 142.1, 146.3, 169.7, 189.4. **MS** *m/z* (%): 415.6 (11.8, M^+).

1-(3,4-Dimethoxyphenyl)-3-oxo-3-(p-tolyl)propyl morpholine-4-carbodithioate (23):

^{1}H-NMR (DMSO-d_6); δ 1.03 (s, 3H, CH_3), 2.39 (d, 2H, *J* = 3.0, $\underline{CH_2}$- C=O), 3.45 – 3.48 (m, 8H, morpholine-H), 3.84 (s, 3H, OCH_3), 3.99 (s, 3H, OCH_3), 4.28 (t, 1H, *J* = 9.5, benzylic-H), 7.02 (d, 2H, *J* = 8.0, Ar-H), 7.37 (d, 2H, *J* = 8.5, Ar-H), 7.52 (s, 1H, Ar-H), 8.05 (d, 2H, *J* = 8.5, Ar-H). **^{13}C-NMR** δ 22.7, 38.4, 50.9, 52.7, 53.6, 55.9, 56.3, 63.9, 65.7, 117.6, 119.4, 120.4, 124.0, 127.3, 128.4, 129.1, 133.4, 134.8, 136.7, 139.6, 145.1, 174.8, 183.4. **IR** (cm $^{-1}$): 1530 (N-CS), 1005 (C-S), **MS** *m/z* (%): 445.6 (35.1, M^+).

3-Oxo-3-(p-tolyl)-1-(3,4,5-trimethoxyphenyl)propyl morpholine-4-carbodithioate (24):

^{1}H-NMR (DMSO-d_6); 1.05 (s, 3H, CH_3), 2.40 (d, 2H, *J* = 3.0, $\underline{CH_2}$- C=O), 3.07 (t, 4H, *J* = 9.5, morpholine-H), 3.49 (s, 3H, OCH_3), 3.70 (s, 3H, OCH_3), 3.73 (t, 4H, *J* = 9.5, morpholine-H), 3.85 (s, 3H, OCH_3), 4.28 (t, 1H, *J* = 9.0, benzylic-H), 7.22 (s, 1H, Ar-H), 7.37 (d, 2H, *J* = 8.0, Ar-H), 7.66 (s, 1H, Ar-H), 8.07 (d, 2H, *J* = 8.0, Ar-H). **^{13}C-NMR** δ 22.1, 38.7, 49.9, 50.4, 52.3, 55.6, 56.7, 59.1, 62.1, 64.9, 118.1, 120.4, 122.1, 126.7, 129.4, 132.0, 133.8, 135.1, 136.2, 137.5, 140.1, 145.3, 168.2, 179.4. **MS** *m/z* (%): 475.6 (10.7, M^+).

3-(4-Methoxyphenyl)-3-oxo-1-(p-tolyl)propyl morpholine-4-carbodithioate (25):

^{1}H-NMR (DMSO-d_6); δ 2.23 (s, 3H, CH_3), 2.34 (d, 2H, *J* = 1.5, $\underline{CH_2}$- C=O), 3.34-3.48 (m, 8H, morpholine-H), 3.86 (s, 3H, OCH_3), 4.29 (t, 1H, *J* = 9.5, benzylic-H), 7.07 (d, 2H, *J* = 6.5, Ar-H), 7.27 (d, 2H, *J* = 8.0, Ar-H), 7.77 (d, 2H, *J* = 8.0, Ar-H), 8.15 (d, 2H, *J* = 9.5, Ar-H). **^{13}C-NMR** δ 20.6, 38.9, 50.1, 51.3, 53.7, 55.7, 63.0, 64.7, 120.4, 122.1, 123.9, 126.8, 129.8, 132.5, 136.2, 144.2, 146.1, 150.8, 152.6, 157.1, 169.5, 189.0. **MS** *m/z* (%): 415.6 (24.8, M^+).

1-(4-Chlorophenyl)-3-(4-methoxyphenyl)-3-oxopropyl morpholine-4-carbodithioate (26):

^{1}H-NMR (DMSO-d_6); δ 2.77 (d, 2H, *J* = 1.5, $\underline{CH_2}$- C=O), 3.46 - 3.55 (m, 8H, morpholine-H), 3.85 (s, 3H, OCH_3), 4.28 (t, 1H, *J* = 9.5, benzylic-H), 7.08 (d, 2H, *J* = 8.5, Ar-H), 7.51 (d, 2H, *J* = 9.0, Ar-H), 7.91 (d, 2H, *J* = 8.0, Ar-H), 8.16 (d, 2H, *J* = 8.5, Ar-H). **^{13}C-NMR** δ 37.1, 49.3, 51.8, 54.9, 55.6, 62.4,

66.9, 119.0, 126.4, 128.3, 129.0, 131.2, 133.7, 135.8, 137.0, 138.6, 139.2, 143.2, 148.1, 159.5, 173.0. **MS** *m/z* (%): 435.9 (17.4, M^+).

1,3-Bis(4-methoxyphenyl)-3-oxopropyl morpholine-4-carbodithioate (27):

^{1}H-NMR (DMSO-d_6); δ 2.87 (d, 2H, *J* = 1.5, $\underline{CH_2}$- C=O), 3.48 (t, 4H, *J* = 9.5, morpholine-H), 3.61 (t, 4H, *J* = 9.5, morpholine-H), 3.81 (s, 3H, OCH_3), 3.85 (s, 3H, OCH_3), 4.29 (t, 1H, *J* = 10.0, benzylic-H), 6.99 (d, 2H, *J* = 7.0, Ar-H), 7.08 (d, 2H, *J* = 9.0, Ar-H), 7.84 (d, 2H, *J* = 8.0, Ar-H), 8.15 (d, 2H, *J* = 8.5, Ar-H). **^{13}C-NMR** δ 38.2, 47.5, 50.4, 53.7, 55.5, 57.6, 63.9, 66.0, 122.0, 124.7, 126.3, 129.4, 133.2, 134.1, 136.8, 137.6, 139.6, 144.3, 148.5, 155.4, 176.3, 190.6. **MS** *m/z* (%): 431.6 (13.3, M^+).

1-(3,4-Dimethoxyphenyl)-3-(4-methoxyphenyl)-3-oxopropyl morpholine-4-carbodithioate (28):

^{1}H-NMR (DMSO-d_6); δ 3.22 (d, 2H, $\underline{CH_2}$- C=O), 3.42 – 3.48 (m, 8H, morpholine-H), 3.81 (s, 3H, OCH_3), 3.86 (s, 3H, OCH_3), 3.91 (s, 3H, OCH_3), 4.28 (t, 1H, *J* = 10.0, benzylic-H), 7.01 (d, 2H, *J* = 7.5, Ar-H), 7.08 (d, 2H, *J* = 7.5, Ar-H), 7.67 (s, 1H, Ar-H), 8.17 (d, 2H, *J* = 10.5, Ar-H). **^{13}C-NMR** δ 36.2, 45.1, 49.7, 52.2, 55.5, 57.3, 59.8, 63.0, 66.8, 124.6, 125.4, 128.1, 130.8, 134.9, 135.0, 137.2, 139.0, 144.4, 145.6, 148.8, 150.7, 1168.4, 179.2. **IR** (cm^{-1}): 1520 (N-CS), 1010 (C-S), **MS** *m/z* (%): 461.6 (9.8, M^+).

3-(4-Methoxyphenyl)-3-oxo-1-(3,4,5-trimethoxyphenyl)propylmorpholine-4-carbodithioate(29):

^{1}H-NMR (DMSO-d_6); δ 2.85 (d, 2H, *J* = 7.5, $\underline{CH_2}$- C=O), 3.43 (t, 4H, *J* = 9.0, morpholine-H), 3.59 (t, 4H, *J* = 8.5, morpholine-H), 3.69 (s, 3H, OCH_3), 3.86 (s, 9H, OCH_3), 4.28 (t, 1H, *J* = 9.5, benzylic-H), 7.10 (d, 2H, *J* = 9.0, Ar-H), 7.24 (s, 1H, Ar-H), 7.66 (s, 1H, Ar-H), 8.16 (d, 2H, *J* = 8.5, Ar-H). **^{13}C-NMR** δ 30.4, 45.4, 50.8, 52.0, 55.6, 57.8, 60.2, 62.7, 65.1, 69.4, 114.2, 117.3, 119.0, 123.6, 127.2, 128.5, 133.4, 137.0, 144.2, 147.1, 149.2, 153.6, 158.2, 168.4. **MS** *m/z* (%): 491.6 (17.2, M^+).

4.1.2 1-(Substituted phenyl)-3-oxo-3-(4-substituted phenyl)propyl 4-benzylpiperazine-1-carbodithioate **(30-39).**

A mixture of carbondisulfide (0.15 ml, 2.5 mM) and chalcone **8-17** (2.5 mM) was dissolved in dichloromethane (10 ml) and the solution was cooled to 0 ^oC in an ice bath. 1-Benzyl piperazine (0.39 g, 2.25 mM) was slowly added and the reaction mixture was stirred at 0 ^oC for 30 min. the reaction procedures were continued as under **20-29** (Table 1).

3-Oxo-1,3-di-p-tolylpropyl 4-benzylpiperazine-1-carbodithioate (30):

^{1}H-NMR (DMSO-d_6); δ 2.34 (s, 3H, CH_3), 2.39 (s, 3H, CH_3), 2.54 (d, 2H, *J* = 7.5, $\underline{CH_2}$- C=O), 3.10 (t, 4H, *J* = 4.5, piperazine-H), 3.52 (t, 4H, *J* = 6.5, piperazine-H), 3.56 (s, 2H, benzylic-H), 4.36 (t, 1H,

J = 7.5, benzylic-H), 7.24 (d, 2H, *J* = 9.0, Ar-H), 7.28-7.33 (m, 5H, Ar-H), 7.40 (d, 2H, *J* = 8.5, Ar-H), 7.77 (d, 2H, *J* = 7.5, Ar-H), 8.06 (d, 2H, *J* = 8.5, Ar-H). **^{13}C-NMR** δ 21.3, 21.8, 37.0, 49.1, 52.7, 52.9, 53.4, 53.8, 66.2, 124.8, 125.3, 126.2, 128.9, 132.7, 135.0, 138.6, 141.6, 144.0, 144.2, 145.3, 146.2, 147.9, 148.6, 149.5, 151.0, 155.3, 158.7, 169.0, 187.4.

1-(4-Methoxyphenyl)-3-oxo-3-(p-tolyl)propyl 4-benzylpiperazine-1-carbodithioate (31):

^{1}H-NMR (DMSO-d_6); δ 2.29 (s, 3H, CH_3), 2.56 (d, 2H, $\underline{CH_2}$- C=O), 3.14 – 3.37 (m, 8H, piperazine-H), 3.72 (s, 2H, benzylic-H), 4.26 (t, 1H, *J* = 7.0, benzylic-H), 7.21 (d, 2H, *J* = 8.5, Ar-H), 7.29-7.35 (m, 5H, Ar-H), 7.42 (d, 2H, *J* = 8.5, Ar-H), 7.60 (d, 2H, *J* = 8.0, Ar-H), 8.10 (d, 2H, *J* = 8.5, Ar-H). **IR** (cm $^{-1}$): 1525 (N-CSS), 1015 (C-S), **MS** *m/z* (%): 508.8 (23.8, M^+).

1-(4-Chlorophenyl)-3-oxo-3-(p-tolyl)propyl 4-benzylpiperazine-1-carbodithioate (32):

^{1}H-NMR (DMSO-d_6); δ 2.21 (s, 3H, CH_3), 2.54 (d, 2H, $\underline{CH_2}$- C=O), 3.11 – 3.33 (m, 8H, piperazine-H), 3.43 (s, 2H, benzylic-H), 3.80 (s, 3H, OCH_3), 4.25 (t, 1H, *J* = 7.5, benzylic-H), 7.07 (d, 2H, *J* = 8.0, Ar-H), 7.25 - 7.31 (m, 5H, Ar-H), 7.50 (d, 2H, *J* = 8.5, Ar-H), 7.66 (d, 2H, *J* = 8.0, Ar-H), 8.08 (d, 2H, *J* = 8.0, Ar-H). **^{13}C-NMR** δ 20.4, 37.6, 42.1, 53.0, 53.4, 53.7, 53.9, 55.6, 62.3, 123.4, 124.6, 126.1, 127.3, 130.0, 133.8, 134.2, 136.2, 139.9, 140.2, 141.8, 142.9, 144.8, 146.0, 148.7, 149.2, 153.7, 155.3, 167.9, 187.3. **MS** *m/z* (%): 504.7 (6.7, M^+).

1-(3,4-Dimethoxyphenyl)-3-oxo-3-(p-tolyl)propyl 4-benzylpiperazine-1-carbodithioate (33):

^{1}H-NMR (DMSO-d_6); δ 2.25 (s, 3H, CH_3), 2.49 (d, 2H, *J* = 5.5, $\underline{CH_2}$- C=O), 3.41-3.47 (m, 8H, piperazine-H), 3.49 (s, 2H, benzylic-H), 3.80 (s, 3H, OCH_3), 3.85 (s, 3H, OCH_3), 4.29 (t, 1H, *J* = 6.5, benzylic-H), 7.21 (d, 2H, *J* = 8.0, Ar-H), 7.30-7.33 (m, 5H, Ar-H), 7.52 (d, 2H, *J* = 8.5, Ar-H), 7.78 (s, 1H, Ar-H), 8.05 (d, 2H, *J* = 7.5, Ar-H). **IR** (cm $^{-1}$): 1517 (N-CS), 1020 (C-S)**MS** *m/z* (%): 534.7 (19.3, M^+).

3-Oxo-3-(p-tolyl)-1-(3,4,5-trimethoxyphenyl)propyl 4-benzylpiperazine-1-carbodithioate(34):
^{1}H-NMR (DMSO-d_6); δ 2.20 (s, 3H, CH_3), 2.45 (d, 2H, *J* = 5.5, $\underline{CH_2}$- C=O), 3.22 - 3.36 (m, 8H, piperazine-H), 3.80 (s, 3H, OCH_3), 3.88 (s, 3H, OCH_3), 3.90 (s, 3H, OCH_3), 3.96 (s, 2H, benzylic-H), 4.25 (t, 1H, *J* = 6.5, benzylic-H), 7.05 (d, 2H, *J* = 8.0, Ar-H), 7.22-7.37 (m, 5H, Ar-H), 7.58 (s, 1H, Ar-H), 7.73 (s, 1H, Ar-H), 8.08 (d, 2H, *J* = 7.5, Ar-H). **^{13}C-NMR** δ 23.1, 36.8, 49.2, 52.7, 53.0, 53.6, 54.0, 55.5, 56.7, 60.1, 63.8, 123.7, 125.7, 127.4, 130.4, 133.6, 137.2, 139.0, 140.0, 141.5, 143.5, 142.8, 144.7, 146.3, 147.2, 149.1, 152.2, 155.6, 157.3, 164.2, 184.0. **MS** *m/z* (%): 564.8 (12.4, M^+).

3-(4-Methoxyphenyl)-3-oxo-1-(p-tolyl)propyl 4-benzylpiperazine-1-carbodithioate (35):

^{1}H-NMR (DMSO-d_6); δ 2.25 (s, 3H, CH_3), 2.43 (d, 2H, *J* = 6.0, $\underline{CH_2}$- C=O), 3.39 -3.48 (m, 8H, piperazine-H), 3.86 (s, 3H, OCH_3), 4.00 (s, 2H, benzylic-H), 4.30 (t, 1H, *J* = 6.5, benzylic-H), 7.07 (d, 2H, *J* = 7.5, Ar-H), 7.25-7.32 (m, 5H, Ar-H), 7.76 (d, 2H, *J* = 8.5, Ar-H), 7.68 (d, 2H, *J* = 8.0, Ar-H), 8.15 (d, 2H, *J* = 7.5, Ar-H). **^{13}C-NMR** δ 22.4, 37.2, 50.1, 52.6, 52.9, 53.7, 54.0, 55.6, 62.9, 119.2, 122.8, 124.5, 125.9, 126.8, 128.0, 133.4, 135.0, 137.5, 138.1, 139.9, 140.0, 142.1, 144.2, 145.2, 146.3, 148.1, 150.9, 157.6, 175.8. **IR** (cm $^{-1}$): 1535 (N-CS), 1018 (C-S) **MS** *m/z* (%): 504.7 (31.7, M^+).

1,3-bis(4-Methoxyphenyl)-3-oxopropyl 4-benzylpiperazine-1-carbodithioate (36):

^{1}H-NMR (DMSO-d_6); δ 2.49 (d, 2H, $\underline{CH_2}$- C=O), 3.34 - 3.44 (m, 8H, piperazine-H), 3.86 (s, 3H, OCH_3), 4.02 (s, 2H, benzylic-H), 4.29 (t, 1H, benzylic-H), 7.06 (d, 2H, *J* = 7.5, Ar-H), 7.23-7.31 (m, 5H, Ar-H), 7.52 (d, 2H, *J* = 8.0, Ar-H), 7.91 (d, 2H, *J* = 8.0, Ar-H), 8.17 (d, 2H, *J* = 7.0, Ar-H). **^{13}C-NMR** δ 36.2, 49.3, 53.1, 53.3, 54.3, 54.8, 55.6, 63.0, 120.3, 120.9, 122.4, 123.6, 125.2, 127.8, 129.2, 133.1, 135.6, 137.5, 138.5, 140.2, 141.0, 144.9, 145.7, 146.6, 148.7, 149.2, 151.1, 168.9. **MS** *m/z* (%): 524.1 (9.2, M^+).

1-(4-Chlorophenyl)-3-(4-methoxyphenyl)-3-oxopropyl4-benzylpiperazine-1-carbodithioate(37):
^{1}H-NMR (DMSO-d_6); δ 2.48 (d, 2H, $\underline{CH_2}$- C=O), 3.11 (t, 4H, piperazine-H), 3.52 (t, 4H, piperazine-H), 3.58 (s, 2H, benzylic-H), 3.80 (s, 3H, OCH_3), 3.86 (s, 3H, OCH_3), 4.33 (t, 1H, benzylic-H), 7.06 (d, 2H, *J* = 7.5, Ar-H), 7.25-7.34 (m, 5H, Ar-H), 7.68 (d, 2H, *J* = 8.5, Ar-H), 7.85 (d, 2H, *J* = 8.0, Ar-H), 8.16 (d, 2H, *J* = 7.5, Ar-H). **^{13}C-NMR** δ 37.2, 48.9, 53.7, 53.8, 54.2, 54.6, 55.6, 56.1, 64.2, 120.6, 122.5, 125.7, 126.2, 129.4, 130.0, 131.2, 133.8, 138.7, 140.0, 141.0, 141.8, 143.2, 144.7, 145.6, 147.3, 149.8, 150.6, 157.4, 169.2. **IR** (cm $^{-1}$): 1535 (N-CS), 1025 (C-S), **MS** *m/z* (%): 520.71 (15.2, M^+).

1-(3,4-Dimethoxyphenyl)-3-(4-methoxyphenyl)-3-oxopropyl4-benzylpiperazine-1carbodithioate (38):

^{1}H-NMR (DMSO-d_6); δ 2.49 (d, 2H, $\underline{CH_2}$- C=O), 3.22-3.41 (m, 8H, piperazine-H), 3.80 (s, 3H, OCH_3), 3.86 (s, 6H, OCH_3), 4.22 (s, 2H, benzylic-H), 4.41 (t, 1H, benzylic-H), 7.01 (d, 2H, *J* = 8, Ar-H), 7.23-7.36 (m, 5H, Ar-H), 7.38 (d, 2H, *J* = 8.5, Ar-H), 7.52 (s, 1H, Ar-H), 8.17 (d, 2H, *J* = 7.5, Ar-H). **MS** *m/z* (%): 550.7 (20.8, M^+).

3-(4-Methoxyphenyl)-3-oxo-1-(3,4,5-trimethoxyphenyl)propyl-4-benzylpiperazine-1-carbodithioate (39):

^{1}H-NMR (DMSO-d_6); δ 2.54 (d, 2H, $\underline{CH_2}$- C=O), 3.10 (t, 4H, piperazine-H), 3.52 (t, 4H, piperazine-H), 3.53 (s, 2H, benzylic-H), 3.69 (s, 3H, OCH_3), 3.85 (s, 3H, OCH_3), 3.86 (s, 6H, OCH_3), 4.21 (t, 1H,

benzylic-H), 7.06 (d, 2H, *J* = 7.0, Ar-H), 7.21 (s, 1H, Ar-H), 7.24-7.34 (m, 5H, Ar-H), 7.87 (s, 1H, Ar-H), 8.16 (d, 2H, *J* = 8.5, Ar-H). **^{13}C-NMR** δ 36.5, 49.8, 53.1, 53.5, 53.7, 54.0, 55.6, 56.4, 57.3, 60.2, 62.3, 120.3, 122.4, 124.1, 126.8, 127.8, 130.1, 131.4, 133.0, 136.7, 141.7, 143.7, 144.2, 146.7, 148.9, 150.1, 155.2, 168.9, 172.0. **IR** (cm $^{-1}$): 1515 (N-CS), 1009 (C-S) **MS** *m/z* (%): 580.7 (13.2, M^+).

4.2 Determination of *in vitro* antimicrobial activity

The primary screen was carried out using the agar disc-diffusion method[1] using Müller-Hinton agar medium. Sterile filter paper discs (8 mm diameter) were moistened with the compound solution in dimethylsulphoxide of specific concentration 200 µg/disc, the antibacterial antibiotic Colistin (200 µg/disc) was carefully placed on the agar cultures plates that had been previously inoculated separately with the microorganisms. The plates were incubated at 37 ^{o}C, and the diameter of the growth inhibition zones were measured after 24 hours including disc diameter. The Minimal inhibitory concentrations (MIC) and the minimal bactericidal concentrations (MBC) for the compounds **22, 24, 25. 26, 27, 33, 35, 36 and 37** in comparison with the broad spectrum antibacterial drug, Colistin against selected multidrug-resistant *Gram negative* clinical isolate, *Pseudomonas aeruginosa* (Ps12) and *Klebsiella pneumoniae* (K4) were carried out using the microdilution susceptibility method in Müller-Hinton Broth. The antibacterial drug, colistin, was dissolved in dimethylsulphoxide at concentration of 64 µg/ml. The twofold dilutions of the solution were prepared (64, 32, …, 0.5 µg/ml). The microorganism suspensions at 10^6 CFU/ml (colony forming unit/ml) concentrations were inoculated to the corresponding wells. The plates were incubated at 37 ^{o}C for 24 hours. The MIC values were determined as the lowest concentration that inhibited the growth of the microorganism as detected by unaided eye and the MBC values were determined by the lowest concentration that killed of the microorganism by re-cultured on solid medium to verify the absence of growth.[24-25]

4.3 Colourimetric assay for DNA binding affinity

DNA methyl green (20 mg) was suspended in 100 ml of 0.05 M Tris-HCl buffer (pH 7.5) containing 7.5 mM $MgSO_4$; the mixture was stirred at 37 °C with a magnetic stirrer for 24 h. Test samples 10,100, 1000 mg) were dissolved in ethanol in Ependoff tubes, solvent was removed under vacuum, and 200 µl of the DNA/methyl green solution were added to each tube. Samples were incubated in the dark at ambient temperature. After 24 h, the final absorbance of the samples was determined at 642.5-645 nm. Readings were corrected for initial absorbance and normalized as the percentage of the untreated standard using Ethidium bromide as positive control. [18, 26].

4.4 Molecular modelling study

Initial structures for the active molecule were constructed Mechanics (MM) calculations in vacuo, bond dipole option for electrostatics, Polake–Ribiere algorithm, and Root Mean Square Deviation (RMSD) gradient of 0.01 kcal/mol conformational searching in torsional space was performed using the multiconformer method. Energy minima for the above compounds were determined by a semi-empirical method AM1 (as implemented in MOE, 2009.10). The three-dimensional structures of the substituted dithiocarbamate chalcone derivatives, which presented best and worst biological profiles, in their neutral forms were constructed using the MOE of Chemical Computing Group Inc software. Lowest energy conformer of each new analogue 'global-minima' was docked into PEA transeferase enzyme-binding domain. Enzyme structure starting coordinate code ID 5FGN was obtained from the Protein Data Bank of Brookhaven National Laboratory [23]. All the hydrogens were added and enzyme structure was subjected to a refinement protocol in which the constraints on the enzyme were gradually removed and minimized until the Root Mean Square Deviation (RMSD) gradient was 0.01 kcal/mol A. The energy minimization was carried out using the molecular mechanics force field 'AMBER.' The energy-minimized structure was used for molecular modeling studies keeping all the heavy atoms fixed until a RMSD gradient of 0.05 kcal/ mol/ A˚ was reached. Ligand structures were built with MOE and minimized using the Molecular Mechanics Force Field (MMFF94x) forcefield until a RMSD gradient of 0.05 kcal/ mol/A˚ was reached. For each of chalcone analogue, energy minimizations were performed using 1000 steps of steepest descent, followed by conjugate gradient minimization to a RMSD energy gradient of 0.01 Kcal/mol/ Å. The active site of the enzyme was defined using a radius of 10.0 Å around selected active site for PEA transferase enzyme. Energy of binding was calculated as the difference between the energy of the complex and individual energies of the enzyme and ligand . The docking was performed using the alpha triangle placement method and the London dG scoring method. 300 results for each ligand were generated, discarding the results with a RMSD value>3 A˚.19 the best scored result of the remaining conformations for each ligand was further analyzed. The protein/ligand complexes were minimized using the MMFF94x force field, until a RMSD gradient of 0.1 kcal mol/A˚ was reached [27-32].

4.5 ADMET analysis

The pharmacokinetic properties of the most active compounds were calculated theoretically by the aid of online PreADMET database. The most important parameters calculated are, HIA: Human Intestinal Absorption, PPB: plama protein binding, BBB: permeability to the blood brain barrier, MDCK: Maden Darby Canine Kidney. When the cell permeability is < 4 nm/s indicates low permeability, when it is 4-70 indicates medium permeability, if > 70 nm/s indicates high permeability. PPB indicates the action,

activity and efficacy of the tested compounds. The drug should not bind strongly to the PP to promote good diffusion and transport to the agent through the target to exert its action when the value is > 90 % indicates the strong binding with the plasma protein.

5 Acknowledgements

The authors would like to extend their sincere appreciation to the Deanship of Scientific Research at King Saud University for its funding of this research through the Research Group Project no. RG-1439-010

6 Declarations

The authors report no declarations of interest.

T. El Malah, H.F. Nour, A. A. Nayl, R. A. Elkhashab, F.M.E. Abdel-Megeid, M.M. Ali, Anticancer evaluation of tris(triazolyl)triazine derivatives generated via click chemistry. Austr. J. Chem. 69(8) (2016) 905-910

7 References

1- K.S Kaye, J.J Engemann, H.S Fraimow, E. Abrutyn, Pathogens resistant to antimicrobial agents: epidemiology, molecular mechanisms, and clinical management. Infect.Dis,Clin. NorthAm, 18 (2004) 467.

2- M. Stavri, L. J Piddock, S. Gibbons, Novel inhibitory activity of the Staphylococcus aureus NorA efflux pump by a kaempferol rhamnoside isolated from Persea lingue Nees J. Antimicrob. Chemother. 59 (2007) 1247.

3- H. A Junio, A. A Sy-Cordero, K. A Ettefagh, J. T. Burns, K. T Micko, T. N. Graf, J. Richter, R. E. Cannon, N. H. Oberlies, N. B. J Cech,. Isolation of berberine tannate using a chromatography activity-guided fractionation from root bark of Berberis hispanica Boiss. & Reut. Nat. Prod. 74, 2011; 1621.

4- S. Biswas, J.M Brunel, J. C Dubus, M. Reynaud-Gaubert, J.M. Rolain,, Colistin: an update on the antibiotic of the 21st century *Expert Rev. Anti. Infect. Ther.* 2012;10:917-934.

5- D.K Mahapatra, S.K. Bharti, V. Asati. Chalcone scaffolds as antiinfective agents; Structural and Molecular target perspectives. Eur. J. Med. Chem. 11 (2015) 496-524.

6- D.L Batovska, I.T. Todorova, Trends in utilization of the pharmacological potential of chalcones. *Curr. Clin.Pharmacolo.,* 5 (2010) 1-29.

7- A. H. Qasemi, J. Mansouri, Valizadeh, Antimicrobial activity of dithiocarbamate sodium salts and their Zn (II) and Ni (II) complexes Research in Pharmaceutical Sciences, 7(5) (2012)

8- N. A. J. Ibrahim, B. N. Ibrahim. Synthesis, structural and antibacterial studies of new dithiocarbamate complexes of Sb(III) and Bi(III) The Malaysian Journal of Analytical Sciences, 18 (2) (2014) 251 – 259.

9- C. L. Donnici, L. J. Nogueira, Araujo M. H., S. R. Oliveira, T. F. F. Magalhães, M.T.P Lopes, A. C. Araújo e Silva, A. M. da Costa, F. Cleide, V. B. Martins, M. A. Stoianoff. *In Vitro* Studies of the Activity of Dithiocarbamate Organoruthenium Complexes against Clinically Relevant Fungal Pathogens Molecules 19 (2014) 5402-5420; doi:10.3390/molecules19045402

10- K. S. Kim, D. H. Oh, H. M. Choi, J.S. Bang, C.J. Ryu, J.H.Kim, M.C. Yoo, H.I. Yang. Pyrrolidine dithiocarbamate, a NF-kappaB inhibitor, upregulates MMP-1 and MMP-13 in IL-1beta-stimulated rheumatoid arthritis fibroblast-like synoviocytes. Eur. J. Pharmacol., 613 (**2009**) 167.

11- H. Imamura, N. Ohtake, H. Jona, A. Shimizu, M. Moriya, H. Sato, Y. Sugimoto, C. Ikeura, H. Kiyonaga, M. Nakano, R. Nagano, S. Abe, K. Yamada, T. Hashizume, H. Morishima, Dicationic dithiocarbamate carbapenems with anti-MRSA activity. Bioorg. Med. Chem., 9 (2001) 1571–1578

12- N. Lal, Dithiocarbamates: A Versatile Class of Compounds in Medicinal Chemistry Chemistry & Biology Interface, 4 (2014) 321-340

13- S. M. El-Messery, E. E. Habib, S.T.A. Al-Rashood, G. S. Hassan, Synthesis, Antimicrobial , Antibiofilm Evaluation and Molecular Modeling Study of New Chalcone Linked Amines Derivatives Journal of Enzyme Inhibition and Medicinal chemistry 33(1) (2018) 818–832.

14- R. Al-Harbi, M. Shaaban, R. Al-wegaisia, F. Moharram, O. Abd El-Rahmane, S. M. El-Messery. Antimicrobial Activity and Molecular Docking of Tannins from Pimenta dioica Letters in Drug Design & Discovery 14 (2017).

15- G. S. Hassan, S. M. El-Messery, A. Abbas. Synthesis and anticancer activity of new thiazolo[3,2-*a*]pyrimidines: DNA binding and molecular modeling study, Bioorganic Chemistry.74 (2017) 41-52.

16- S. A. El-Mowafy, K. H. Abd El Galil, S. M. El-Messery, and M. I. Shaaban. Aspirin an Efficient Inhibitor of Quorum Sensing, Virulence and Toxins of Pseudomonas aeruginosa, Microbial pathogenesis 74 (2014) 25-32.

17- (a) B.S. Holla, B.S. Rao, B.K. Sarojini, P.M. Akberali , One pot synthesis of thiazolodihydro-pyrimidinones and evaluation of their anticancer activity, Eur. J. Med. Chem. 39 (2004) 777–783. (b) I. Karaman, H. Gezegen, M.B. Guerdere, A. Dingil, M. Ceylan, Screening of biological activities of a series of chalcone derivatives against human pathogenic microorganisms, Chem. Biodivers. 7 (2010) 400–408. (c) A. Z. Halimehjani, K. Marjan and A. Ashouri Synthesis of dithiocarbamate by Markovnikov addition reaction in aqueous medium . Green Chem., 12 (2010) 1306–1310.

18- I. H. Eissa, A. M. El-Naggar, M. A. El-Hashash Design, synthesis, molecular modeling and biological evaluation of novel *1H*-pyrazolo[3,4-*b*]pyridine derivatives as potential anticancer agents Bioorganic Chemistry 67 (2016) 43–56.

19- M. Kontoyianni , .L.M. McClellan, G.S. Sokol. Evaluation of docking performance: comparative data on docking algorithms. J. Med. Chem. 47 (2004) 558–565.

20- R. Wang, Y. Lu, S. Wang Comparative evaluation of 11 scoring functions for molecular docking. J Med Chem 46 (2003) 2287–2303.

21- B.D.Needham, M.S. Trent Fortifying the barrier: The impact of lipid A remodelling on bacterial pathogenesis. Nat Rev Microbiol 11(7) (2013) 467–481.

22- S.N. Bartley, C.M. Kahler The glycome of Neisseria spp.: How does this relate to pathogenesis? Pathogenic Neisseria: Genomics, molecular biology, and disease intervention, eds Kahler CM, Davies JK 2014; (Caister Academic Press, Poole, UK), pp 114–145.

23- A Anandan, G L Evans, K. Condic-Jurkic, M. L. O'Mara, M. J. Constance , N. J. Phillips A .Gary, S . Jarvis Siobhan. A. Wills Keith, Isabel Moraes, C. M. Stubbs Kahler and A. Vrielink www.pnas.org/cgi/doi/10.1073/pnas.1612927114.

24- Clinical and Laboratory Standards Institute (CLSI). Performance standards for antimicrobial susceptibility testing, CLSI approved standards M100-S15., Wayne, PA 2008.

25- P. R Murray, E. J Baron, M. A Pfaller, F. C. Tenover, R. H. Yolken, In Manual of Clinical Microbiology; Wood, G. L.; Washington, J. A., Eds. Am. Soc. Microbiol.: Washington D.C. 1995

26- N.S. Burres , A. Frigo, R. R. Rasmussen, J.B. McAlpine.A colorimetric microassay for the detection of agents that interact with DNA. J Nat Prod. 55 (1992) 1582-7.

27- N. L. Allinger, Conformational analysis. 130. MM2. A hydrocarbon force field utilizing V_1 and V_2 torsional terms. *J. Am. Chem.Soc.,* 99 (1977) 8127-8134.

28- S. Profeta, & N. L. Allinger, Molecular mechanics calculations on aliphatic amines. *J. Am. Chem.Soc.,* 107 (*1985)* 1907-1918.

29- S. Kearsley & G. M. Smith, An alternative method for the alignment of molecular structures: maximizing electrostatic and steric overlap. *Tetrahedron Computer Methodol*ogy, 3 (1990) 615-633.

30- P. Labute, C. Williams, M. Feher, E. Sourial, & J. M. Schmidt, Flexible alignment of small molecules. *J. Med. Chem., 2001;*44: 1483-1490.

31- B. J. Stockman, N. R. Nirmala, G. Wanger, T. J. Delcamp, M. T. DeYarman, & J. H. Freisheim, Methotrexate Binds in a Non-Productive Orientation to Human Dihydrofolate Reductase in Solution Based on NMR Spectroscopy. *Federation of European Biochemical Societies Letters,* 283 (1991) 267-269.

32- V. Cody & C. H. Schwalbe, Structural characteristics of antifolate dihydrofolate reductase enzyme interactions. *Crystallography Reviews,* 12 (2006) 301-333.

Captions:

Chart 1: Structures of antimicrobial dithiocarbamates

Chart 2: Representation of different active part of newly synthesized compounds against bacteria Design of active

Scheme 1: Synthesis of the target compounds **20-39**

Table 1: The physiochemical properties of the synthesized compounds **20-39**

Table 2: Antibacterial activity of tested compounds (200 µg/8 mm disc) against selected multidrug-resistant *Gram negative* clinical isolate, *Pseudomonas aeruginosa* (Ps12) and *Klebsiella pneumoniae* (K4).

Table 3: The Minimal Inhibitory Concentrations (MIC, µg/ml) and Minimal Bactericidal Concentrations (MBC µg/ml) of compounds **20, 22, 24, 25. 26, 27, 28 33, 34 35, 36 and 37** in comparison with the broad spectrum antibacterial drug, Colistin against selected multidrug-resistant *Gram negative* clinical isolate, *Pseudomonas aeruginosa* (Ps12) and *Klebsiella pneumoniae* (K4).

Table 4: DNA/methyl green colourimetric assay of the DNA-binding compounds

Figure 1 2D binding mode and residues involved in the recognition of reference cocrystalized ligand in phosphoethanolamine transferase enzyme active site

Figure 2: 2D binding mode and residues involved in the recognition of **20** in phosphoethanolamine transferase enzyme active site.

Figure 3: 2D binding mode and residues involved in the recognition of **22** in phosphoethanolamine transferase enzyme active site .

Figure 4: 2D binding mode and residues involved in the recognition of **24** in phosphoethanolamine transferase enzyme active site

Figure 5: The aligned conformations of the most active compound **24** (IC_{50} 0.004 µM); occupying phosphoethanolamine transferase enzyme active site

Figure 6: 2D binding mode and residues involved in the recognition of **25** in phosphoethanolamine transferase enzyme active site.

Figure 7 : DNA minor groove binding of (a) Distamycin (yellow) with DNA, DNA is shown in ribbon form. Distamycin, is shown in ball and cylinder form. Hydrogen-bonding (HB) interactions of with the DNA bases (dashed lines). Numbers indicate the percent of HB

Figure 8: Lowest energy conformers of active compounds (a) **28** , (b) **34**, and the least active compounds (c) **21** and (d) **31** with balls and cylinders

Figure 9: Close-up view of active candidates **28** (a), **34** (b) and inactive candidates **21** (c), **31** (d) binding in the DNA minor groove, highlighting the "isohelical" conformation of DNA active binders **28** and **34** to fit into minor groove

Research Highlights

- Synthesis of Dithiocarbamate chalcone-based derivatives scaffold.
- Antibacterial screening against selected *Gram negative* bacteria focusing on microbial resistance were performed where most of the compounds showed equal or higher activity than colistin standard.
- Compound **24** proved to be the most active candidate with MIC of 8 µg/ml against both Ps12 and K4 and MBC of 32 µg/ml against Ps12 and 16 µg/ml against K4 respectively.
- .Compounds **28** and **34** were recorded to have DNA binding better than doxurubucin standard with IC_{50} of 27.48 and 30.97 µg/ml respectively
- Compounds **20, 22,24** and **25** had good binding affinity to PEA transferase *via* Thr280, where **28** and **34** showed a clear intercalation between DNA double strands.

Graphical abstract

Targeting Microbial Resistance: Synthesis, Antibacterial Evaluation, DNA Binding and Modeling Study of New Chalcone-Based Dithiocarbamate Derivatives

Marwa Ayman[1], Shahenda M. El-Messery[2#], Elsayed E. Habib[3,4], Sara T. Al-Rashood[5], Abdulrahman A. Almehizia[5], Hamad M. Alkahtani[5], Ghada S. Hassan[6*]

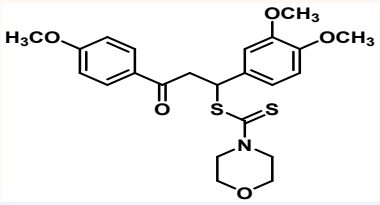

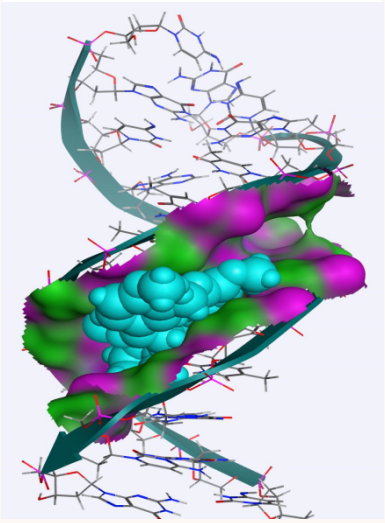

Compound 28

MIC 32 µg/ml

IC_{50} 27.48±1.5 µg/ml

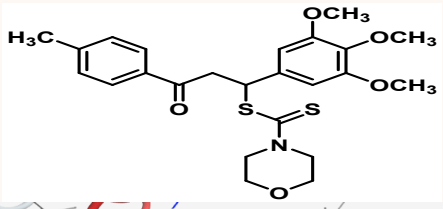

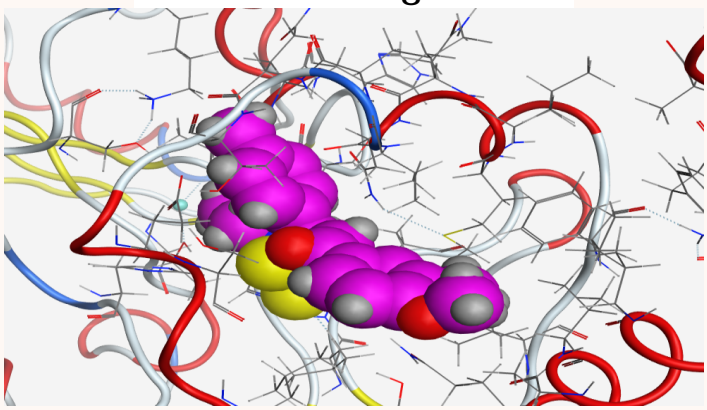

Compound 24 against;

Pseudomonas aeruginosa MIC 8 µg/ml MBC 32 µg/ml

Klebsiella pneumoniae MIC 8 µg/ml MBC 16 µg/ml

Occupying Phoshoehanolamine pocket